Self-energy effects of the optical phonons of heavily doped p-GaAs and p-Ge

Diego Olego and Manuel Cardona
Max-Planck-Institut für Festkörperforschung, Heisenbergstrasse 1, 7000 Stuttgart 80, Federal Republic of Germany
(Received 10 November 1980)

We have studied, using first-order Raman scattering, the self-energy of the long-wavelength transverse-optical phonons of p-GaAs as well as the optical phonons of p-Ge. The phonon Raman lines of p-GaAs are shifted to lower energies and become broadened compared with those of the pure material. They also show an asymmetrical line shape characteristic of a Fano-type discrete-continuum interference. The electronic continuum interacting with the transverse-optical phonons of p-GaAs has been characterized as indirect intraband transitions with initial and final states in the heavy-hole valence band. The phonon Raman lines of p-Ge display effects similar to those of p-GaAs. However, the frequency shifts and broadening depend on the wavelength of the laser light used to excite the spectra. Intra- and inter-valence-band transitions provide the continuum responsible for the Fano asymmetry. The dependence of the self-energy of the phonons on the incident photon energy is attributed to the dispersive nature of the *intraband* electron-phonon coupling with the heavy-hole band. By fitting the frequency shifts of the phonon Raman lines measured for different laser wavelengths to the theory a value of 32 ± 6 eV is obtained for the deformation-potential constant d_0 of Ge.

I. INTRODUCTION

In solids, in particular semiconductors, electronic excitations can interact with phonons. The most general form of interaction is the so-called deformation-potential mechanism. It produces, in heavily doped semiconductors, a renormalization of the frequency as well as the lifetime of the Raman phonons.[1] The frequency shifts can be described as the real part of a phonon self-energy while changes in the lifetimes correspond to its imaginary part. Self-energy effects for optical phonons can be measured by means of first-order Raman scattering. Shifts to lower energies in the position of the phonon Raman lines and a broadening of these lines were reported by Cerdeira and Cardona for n- and p-type Si and p-type Ge with the Fermi level above either the conduction-band minima (n-Si) or below the top of the valence bands (p-Si and p-Ge).[2] Besides frequency shifts and broadening, the first-order Raman lines of heavily doped n- and p-type Si show a Fano asymmetry, characteristic of a coherent discrete-continuum interaction between the one-phonon scattering and a Raman-active continuum of electronic excitations.[3,4] In p-type Si the continuum is provided by direct inter-valence-band transitions from filled states in the light hole band to empty states above the Fermi level in the heavy hole band.[4] In n-type Si it arises from direct electronic transitions between the Δ_1 and Δ_2 conduction-band states, located around the $\langle 0.8,0,0\rangle$ minima.[3] When the energy of the phonon overlaps with the energy of the continuum, interferences of the Raman amplitudes of both kinds of excitations give rise to the observed asymmetric line shapes.[1] Recently a Fano-type asymmetry of the Raman line was reported for photoexcited intrinsic Si.[5] Preliminary results have also shown a Fano-type asymmetry in the one-phonon Raman lines of heavily doped p-GaAs and p-Ge.[6]

In this paper we present a detailed study of the self-energy and Fano-interference phenomena for the long-wavelength optical phonons of heavily doped p-Ge and the transverse-optical phonons (TO phonons) of p-GaAs. In both cases the hole concentrations we are dealing with are such that the Fermi levels lie below the top of the valence bands. The coupling in p-GaAs between the longitudinal-optical phonons (LO phonons) and the free holes has been the subject of a previous publication.[7]

Our results can be summarized as follows: The TO-phonon Raman lines of heavily doped p-GaAs are shifted to lower energies when the free hole concentration exceeds 10^{19} holes cm^{-3}. Besides, the phonon Raman lines show a Fano-type asymmetrical broadening due to the coherent interference with an inter-valence-band electronic Raman scattering which has been reported previously for these samples.[8] Our measurements of the first-order Raman scattering in heavily doped p-Ge reproduce the self-energy effects described in Ref. 2. However, the shift and broadening of the phonon Raman lines of p-Ge depend on the wavelength of the incident laser line, a rather unusual observation in the case of the first-order Raman scattering. The Raman lines of p-Ge display also as in the case of p-type GaAs, a Fano asymmetry. These effects were not investigated in Ref. 2.

The dependence of the energy position of the Raman lines of heavily doped p-Ge on the incident laser energy reveals a strong dispersion of the long-wavelength phonons, which resembles a

Kohn-type anomaly. The coupling of the optical phonons with intraband heavy-hole excitations is responsible for the observed effects. A value of the deformation-potential constant is obtained by fitting the frequency shifts as a function of the phonon wave vectors.

The organization of the paper is as follows: The experimental details are presented in the next section. A brief description of the Fano effect is given in Sec. III in order to develop the formalism needed for the understanding of the experimental results, which are presented and discussed in Sec. IV.

II. EXPERIMENTAL DETAILS

The Raman measurements were performed in the backscattering configuration standard for opaque materials. Several lines of an Ar^+- and Kr^+-ion laser were used to excite the spectra. The scattered light was analyzed with a wave-number driven Spex triple monochromator and detected with an RCA 31034 photomultiplier equipped with photon-counting electronics. The counts were stored on a multichannel analyzer with typical integration times per channel ranging from 2 to 5 sec and a spacing of ~0.2 cm^{-1} between adjacent channels. A neon lamp was used for wavelength reference and calibration purposes.

The samples were cut from Zn-doped GaAs and Ga-doped Ge single crystals. The hole concentrations were determined by means of Hall measurements, of plasma edge measurements in the reflection spectrum, and by measuring the resistivity with a four-probe technique. The relationship between resistivity and free hole concentration was taken from Ref. 9. The hole concentrations as determined by the three different methods agree within 10%. The scattering factor in the expression for the Hall constant is taken equal to one ($R_H=-1/pec$), a fact loosely justified by the equality of the hole concentration with that obtained from the plasma edge measurement.

Surfaces with a (110) orientation, either cleaved or polished and etched with an aqueous solution of NaOCl, were used for the measurements of the transverse-optical phonons of p-GaAs. For this surface orientation, scattering by longitudinal-optical phonons is not allowed by the selection rules of the first-order normal Raman scattering.[10] Cleaved surfaces [(111) orientation] or surfaces polished and etched with Syton [(111) or (100) orientation] were used to measure the Raman scattering by optical phonons in p-Ge. The shapes of the recorded spectra were in all cases independent of the surface preparation (cleaved or polished-etched). For the measurements at low temperature, the samples were glued with silver paste to a copper cold finger which was placed in an evacuated glass Dewar and maintained in contact with a liquid-nitrogen bath.

III. THEORY

In this section we consider the coupling between electron (holes) and optical phonons which takes place through the deformation-potential mechanism. This interaction is responsible not only for the self-energy of the phonons but also for similar renormalization effects on the electronic band states, which show up, for example, in the temperature dependence of the band structure.

To describe the renormalization of phonon frequencies due to the electron-phonon deformation-potential interaction two cases have to be distinguished. When the phonon frequency is very small compared with a typical redistribution time of the electron (holes), the phonons can be considered as a static perturbation similar to an externally applied stress. The renormalization of the phonon frequencies follows from free-energy considerations.[11] Using these arguments the influence of free carriers on the acoustic phonons and on the elastic constants has been quantitatively explained.[12]

On the other hand, when the phonon frequency is comparable with the free-carrier redistribution time, as in the case of the optical phonons, the electron-phonon interaction has to be treated in a quantum-mechanical way allowing for a decay of the phonons into electron-hole excitations and vice versa.[12] Thus the renormalization of high-energy phonons results from a change in the phonon self-energy due to a dynamical coupling with the free carriers.

If the two interacting elementary excitations, in our case TO phonon and electron-hole pairs, are simultaneously Raman active and if the frequency of the phonon overlaps with the energy of the electronic excitations, the phonon Raman line may depart from the usual Lorentzian shape in pure materials.[13] The change from symmetrical to asymmetrical phonon line shapes, the so-called Fano effect, was observed with increasing free-carrier concentration in n- and p-type Si.[3,4]

The theory for the interaction of a discrete line with a continuum was treated by Fano.[14] A theory for the asymmetric line shape of the Fano effect in inelastic light scattering experiments, taking into account explicitly the self-energy of the phonons has been developed recently.[3,12] The Raman spectrum is described by the following expression:

$$I(\eta,\tilde{q}) = A\frac{(\tilde{q}+\eta)^2}{1+\eta^2}, \tag{1}$$

where

$$\eta = \hbar \frac{\omega - \Omega_0 - \Delta\Omega}{\Gamma} \tag{2}$$

and

$$\tilde{q} = \frac{VR_p}{\Gamma R_e}. \tag{3}$$

A is a constant. In Eq. (2) Ω_0 represents the phonon frequency of the pure material, $\Delta\Omega$ the renormalization of this frequency due to the electron-phonon interaction in the heavily doped material, and Γ the linewidth. The asymmetry parameter $\tilde{q}$ is related to the electron-phonon matrix element V, the phonon Raman tensor R_p, and the Raman tensor R_e of the electronic excitations. From Eq. (1) it follows that the phonon Raman line shape is more asymmetric the closer the parameter $|\tilde{q}|$ is to unity.

The asymmetry disappears if $\tilde{q}$ is pure imaginary. For the cases of n- and p-type Si $\tilde{q}$ turns out to be basically real. The linewidth Γ can be decomposed in two contributions,

$$\Gamma = \Gamma_0 + \Delta\Gamma, \tag{4}$$

where Γ_0 is the natural linewidth of the phonon Raman line in the pure material and $\Delta\Gamma$ the broadening due to the interaction.

The frequency shift $\Delta\Omega$ is given by the real part of the phonon self-energy:

$$\hbar\Delta\Omega = V^2 \mathrm{P} \int \rho(E') \left(\frac{1}{\hbar\Omega - E'} - \frac{1}{\hbar\Omega + E'} \right) dE', \tag{5}$$

with $\rho(E')$ the combined density of states for the electronic excitations. P means the principal value of the integral. The broadening $\Delta\Gamma$ and the density of states can be expressed by

$$\Delta\Gamma = V^2 \pi \rho(\hbar\Omega). \tag{6}$$

IV. RESULTS AND DISCUSSION

A. p-GaAs

Figure 1 shows typical Raman spectra of the TO phonons (Γ_{15} symmetry) of pure and heavily doped p-type GaAs recorded at 77 K. The zero point on the horizontal energy scale corresponds to the frequency of the TO phonon of pure GaAs (~271 cm^{-1} at 77 K). The phonon Raman lines of the heavily doped material are shifted to lower energies and are asymmetrically broadened compared with that of pure GaAs. They display a weak antiresonance on the high-energy side of the spectrum. The observed asymmetry diminishes with increasing incident photon energy. We were able to measure shifts and broadenings of Raman lines for samples with hole concentrations larger than 4×10^{19} holes cm^{-3}. For samples with lower hole concentrations no difference was detected between their TO-Raman spectra and that of the undoped material.

As was mentioned in the preceding section, the asymmetry in the shape of the phonon Raman line

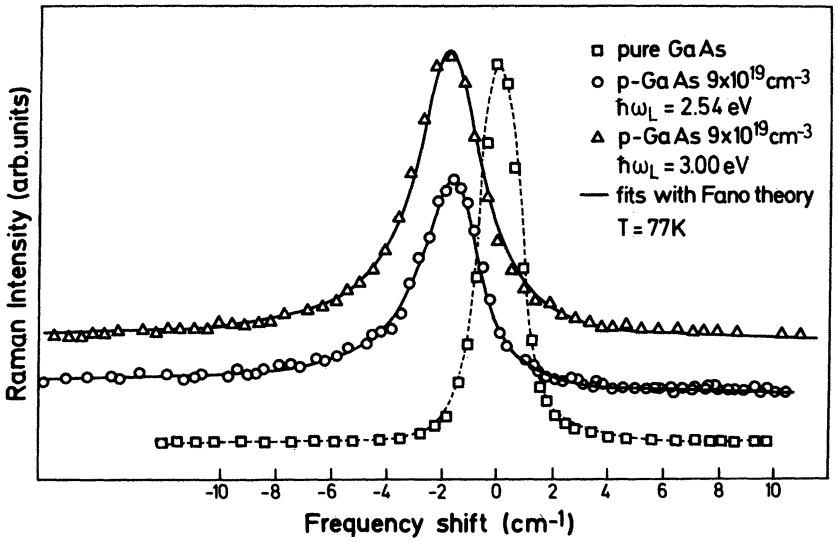

FIG. 1. First-order Raman spectra of the transverse-optical phonons of pure and p-type GaAs recorded at 77 K. The origin on the energy scale was placed at the transverse-optical phonon energy of undoped GaAs (~ 271 cm^{-1} at 77 K). The Raman lines of the heavily doped material are shifted to lower energies and show an asymmetrical line shape. The solid lines represent fits calculated with Eq. (1).

arises from a coherent interference between the discrete phonon line and a continuum of electronic excitations which should also be Raman active. We have already reported intra- and inter-valence-band electronic Raman scattering (ERS) in p-GaAs.[8] For samples with 4×10^{19} and 9×10^{19} holes cm^{-3} intraband electronic Raman scattering of symmetry Γ_{15} was measured in the Stokes spectra at energies around that of the TO phonon. This scattering provides the continuum of electronic excitations necessary to explain the Fano line shape of the TO phonons.

The intraband ERS arises from indirect transitions with initial and final states within the heavy hole band. The breakdown of the wave-vector conservation was attributed to elastic scattering of the photoexcited electrons by ionized Zn impurities. Direct inter-valence-band transitions give a continuum with a threshold at much higher energies than that of the TO phonon (see Fig. 2 in Ref. 8). Thus no interference can take place with these excitations.

On the other hand, the fact that no intraband ERS was detected at the energy of the TO phonon for samples with 1.6×10^{19} holes cm^{-3} agrees with the lack of self-energy effects for this concentration.[8] The experimental Raman lines of Fig. 1 were fitted with Eq. (1). From the fitting procedure the parameters $\tilde{q}$, $\Delta\Omega$, and $\Delta\Gamma=\Gamma-\Gamma_0$ were obtained. Their values are listed in Table I.

The asymmetry parameter $\tilde{q}$ depends on the temperature and on the incident photon energy. With increasing temperature, larger values of $\tilde{q}$ are obtained, i.e., the Raman lines become more symmetric. This behavior can be explained by considering that due to the presence of indirect transitions, a larger amount of intraband ERS of symmetry Γ_1 takes place at higher temperatures,[8] which introduces an extra incoherent channel for the discrete-continuum interaction.[2]

The dependence of $\tilde{q}$ on the incident photon energy results from the resonant behavior of the phonon Raman tensor R_p. In the energy range from 2 to 3 eV it was experimentally determined that R_p increases with increasing energy.[15,16] Owing to the relation (3) between R_p and $\tilde{q}$, an increase in R_p means larger values of $\tilde{q}$ (R_e is only weakly resonant).

The negative sign of $\tilde{q}$ implies different signs for the Raman tensors R_p and R_e since the deformation-potential constant d_0 is positive. The phonon Raman tensor R_p of the optical phonons of the group-IV semiconductors as well as that of the transverse-optical phonons of the III-V compounds is negative,[17] while the Raman tensor R_e of the electronic scattering is positive for the incident photon energies used to perform

TABLE I. Shifts, broadenings, and asymmetry parameters of the Raman lines for heavily doped p-GaAs.

Hole concentration (cm^{-3})	Shifts $\hbar\Delta\Omega$ (cm^{-1})		Broadenings $\Delta\Gamma$ (cm^{-1})		Fano asymmetry parameter $\tilde{q}$									
					2.41 eV		2.54 eV		2.70 eV		3.0 eV		3.05 eV	
	300 K	77 K	300 K	77 K	300 K	77 K	300 K	77 K	300 K	77 K	300 K	77 K	300 K	77 K
4×10^{19}	-1.3 ± 0.2	-1.4 ± 0.2	1.0 ± 0.2	1.0 ± 0.2		-20 ± 3		-20 ± 3						
9×10^{19}	-2.3 ± 0.2	-2.2 ± 0.2	1.7 ± 0.2	1.5 ± 0.2	-17 ± 2	-10 ± 2	-15 ± 2	-9 ± 1	-17 ± 2	-10 ± 1		-18 ± 2		-18 ± 2

the experiments [see Eq. (1) in Ref. 8]. The electronic continuum which interacts with the TO phonon in GaAs has been characterized as indirect intraband excitations within the heavy-hole band. In the model proposed to explain the Stokes shifts of this scattering, it was assumed that the final states for the indirect transitions lie near the Fermi energy.[8] Correspondingly, the combined density of states can be written as follows:

$$\rho(E') = \frac{1}{\pi^4\hbar^6} m_v^3 E_F^{1/2} (E' + E_F)^{1/2}, \tag{7}$$

where m_v is the effective mass of the heavy holes and E_F is the Fermi energy measured from the top of valence bands. Equation (7) represents the convolution of two parabolic densities of states corresponding to the initial and final states. It is very difficult to perform a theoretical estimate of the frequency shift and the broadening from Eqs. (5) and (6) with Eq. (7) for the density of states, as for indirect transitions the matrix element V besides the electron-phonon coupling should include the electron-impurity interaction. No detailed theoretical calculations of this impurity-induced scattering are available at the present, particularly when the screening length is comparable with the distance between the ionized impurities (this is approximately the case in our samples). The same difficulties arose in the study of the coupled plasmon-phonon modes in these materials.[7]

In spite of these difficulties we are able to explain qualitatively the ratio between the broadenings for two different hole concentrations. Assuming that V^2 is nearly the same for both 9×10^{19} and 4×10^{19} holes cm^{-3}, it results from Eqs. (6) and (7) that

$$\frac{\Delta\Gamma_i}{\Delta\Gamma_j} = \left(\frac{E_F^i(E_F^i+\hbar\Omega)}{E_F^j(E_F^j+\hbar\Omega)}\right)^{1/2}. \tag{8}$$

With $\hbar\Omega \simeq 271$ cm^{-1} = 33.6 meV (TO energy at 77 K), $E_F(9\times10^{19}) = 116$ meV (Ref. 18), and $E_F(4\times10^{19}) = 84$ meV (Ref. 18), Eq. (8) gives

$$\frac{\Delta\Gamma(9\times10^{19})}{\Delta\Gamma(4\times10^{19})} = 1.33 \tag{8'}$$

in good agreement with the experimental value of 1.5 ± 0.4 at 77 K (from Table I). The assumption of a V^2 independent of acceptor concentration N_h is easy to justify if one assumes for the impurity a screened Coulomb potential. For $\vec{k}$ transfers in the Coulomb scattering such that $k \lesssim k_{TF}$ (k_{TF} = Thomas-Fermi momentum) V^2 would be expected to be proportional to $N_h N_h^{-2/3} = N_h^{1/3}$. This would introduce another factor of 1.3 in the ratio of Eq. (8') while still preserving the agreement with the experimental findings.

B. *p*-Ge

Figure 2 displays the optical-phonon Raman lines of pure and heavily doped p-Ge with 5.5×10^{19} holes cm^{-3} recorded at 77 K. The origin of energies was taken at the energy of the long-wavelength optical phonon of pure Ge (~303 cm^{-1} at 77 K).

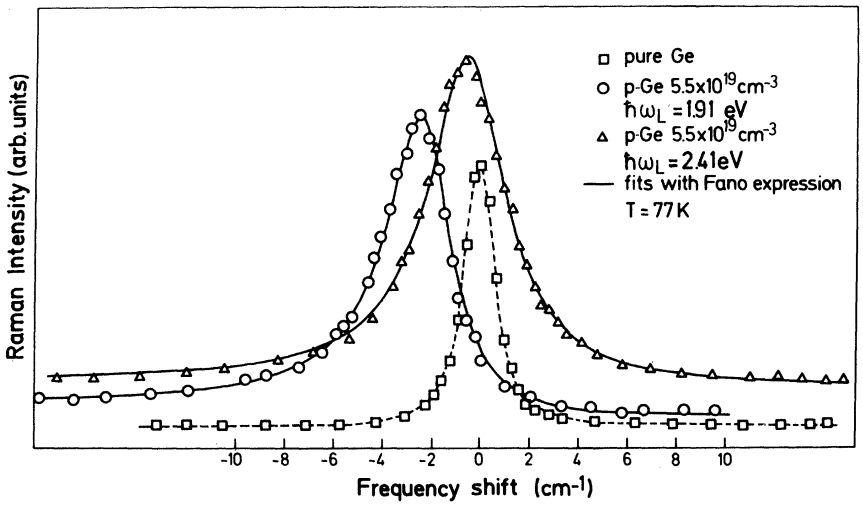

FIG. 2. First-order Raman spectra of the optical phonons of pure Ge and p-Ge with 5.5×10^{19} holes cm^{-3} recorded at 77 K. The origin on the energy scale was placed at the optical-phonon energy of undoped Ge (~303 cm^{-1} at 77 K). As in the case of p-GaAs the Raman lines are shifted to lower energies and asymmetrically broadened. However, the shifts and broadening depend on the incident photon energy. The solid lines represent fits calculated with Eq. (1).

As in the case of p-GaAs, the Raman lines of p-Ge are shifted with respect to that of the pure material and asymmetrically broadened, with antiresonances on the high-energy side of the spectrum. However, the shifts and linewidths of the Raman lines depend on the incident photon energy. This behavior, which was not observed in p-GaAs, is unusual in the first-order Raman scattering by phonons. Similar observations were made with samples of other hole concentrations. Figure 3 shows typical Raman spectra for p-Ge with 2×10^{20} holes cm^{-3}. One may conjecture that the effects observed are connected with dopant concentration gradients near the surface: When the penetration depth of the light changes, the self-energy of the phonons would then change as different hole concentrations are sampled. With this assumption it would be impossible to explain simultaneously the behavior observed for the samples with 5.5×10^{19} and 2×10^{20} holes cm^{-3}. With increasing photon energy the observed self-energies change in opposite directions; however, the penetration depth at 1.91 eV is much smaller than that at 2.41 and 2.54 eV for pure samples, and the slight broadening of the absorption spectrum expected for the heavily doped samples should not change this fact.[19] We also exclude surface damage as a cause of the observed dispersion as no effects are observed for less doped samples.

The solid lines of Figs. 2 and 3 represent fits to the experimental line shapes which were performed with Eq. (1). The values of the parameters $\Delta\Omega$, $\Delta\Gamma$, and $\tilde{q}$ obtained from the fitting procedure are listed in Table II. As already mentioned, the shifts and broadenings of the Raman lines are different for different incident laser energies. For samples with 2.4×10^{19} holes cm^{-3} the Raman lines even appear at higher energies than those for pure Ge when the energy of the incoming photons is larger than 2.3 eV: The self-energy $\Delta\Omega$ is positive as shown in Table II.

In the case of Ge the calculated threshold for direct inter-valence-band transitions lies also above the phonon frequency and one has to invoke indirect transitions to explain the observed Fano-type asymmetry.[12] However, we are not able to characterize the electronic continuum as was possible for p-GaAs. Intra- as well as inter-valence-band transition without wave-vector conservation may provide the continuum which interacts with the phonon.

Both the temperature dependence and the sign of the asymmetry parameter $\tilde{q}$ can be explained following the arguments discussed for p-GaAs. The increase of $\tilde{q}$ with increasing incident photon energy is again related to the resonant behavior of the phonon Raman tensor R_p. In the energy from 1.8 and 2.3 eV R_p shows a resonance which produces the increase of $\tilde{q}$ according to Eq. (3).[20] For energies above 2.3 eV the phonon Raman tensor has an imaginary part[13] which does not seem to interfere coherently with the possible electronic excitations.[12] Thus the phonon Raman lines become more symmetric, meaning larger effective values of $\tilde{q}$.

In the last part of this section we want to discuss in detail the dependence of the frequency shifts $\Delta\Omega$ and broadening $\Delta\Gamma$ on the incident laser energy. In the first-order Raman scattering by phonons, one measures the energy of the optical

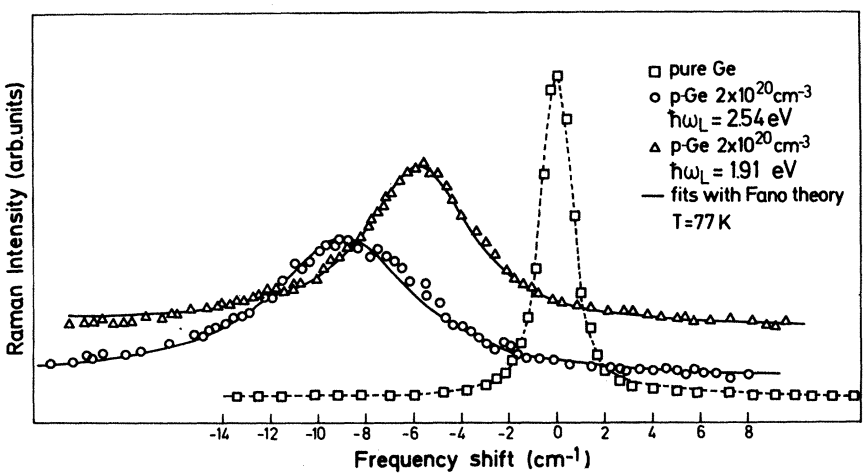

FIG. 3. First-order Raman spectra of the optical phonons of pure Ge and p-Ge with 2×10^{20} holes cm^{-3} recorded at 77 K. The origin on the energy scale was placed at the optical-phonon energy of undoped Ge (~303 cm^{-1} at 77 K). As in the case of p-GaAs the Raman lines are shifted to lower energies and asymmetrically broadened. However, the shifts and broadening depend on the incident photon energy. The solid lines represent fits calculated with Eq. (1).

TABLE II. Shifts, broadenings, and asymmetry parameters of the Raman lines for heavily doped p-Ge for different incident laser energies $\hbar\omega_L$. The experimental error in the determination of the shifts and broadening is ± 0.2 cm^{-1}.

Hole concentration (cm^{-3})	$\hbar\omega_L$ (eV)	Shifts $\hbar\Delta\Omega$ (cm^{-1}) 300 K	77 K	Broadenings $\Delta\Gamma$ (cm^{-1}) 300 K	77 K	Fano asymmetry parameter $\tilde{q}$ 300 K	77 K
2.4×10^{19}	1.83	−0.6	−0.8	1.4	1.1		
	1.92	−0.9	−0.7	1.2	1.3		−25±5
	2.18	−0.1	−0.5	2.2	2		−50±10
	2.41	0.9	0.9	3	2.8		−150±20
	2.54	1	1.3	3.5	4.7		
	2.71	1	0.9	4.2	4.9		
5.5×10^{19}	1.83	−2.2	−2.3	2.4	2.1		
	1.92	−2.1	−2.5	2.4	2.5	−15±2	−9±2
	2.18	−2	−2	3.4	3.1	−50±10	−14±2
	2.41	−1.2	−1.1	3.8	3.5	−80±15	−30±5
	[illegible]4	−1.1	−0.5	5.2	4.9		
	2.71	−0.5	−1.2	6.7	6.8		
2×10^{20}	1.83	−6.8	−7.0	5.6	5.6		
	1.92	−6.5	−6.0	5.4	4.7		−30±10
	2.18	−6.8	−7.4	5.6	6.0		
	2.54	−8.9	−9.1	7.0	8.9		−50±15
	2.71	−8.4	−9.0	8.8	10.2		

phonons with wave vectors near the center of the Brillouin zone.[13] The phonon dispersion curves $\hbar\Omega(\vec{q})$ are nearly flat for wave vectors $\vec{q}\simeq 0$ and consequently the energy position of the phonon Raman line does not normally depend on the incident photon energy. In the case of p-Ge the observed dependence of the position and broadening of the Raman lines on the laser energy reveals a strong dispersion of $\Omega(\vec{q})$ for wave vectors $\vec{q}$ near the Γ point. The relationship between the incident photon energy and the wave vector $\vec{q}$ of the phonon created through the Raman process is given by[10,13]

$$q \simeq 4\pi \frac{n(\lambda)}{\lambda} \tag{9}$$

with $n(\lambda)$ the refractive index at the wavelength λ of the incident laser light and $q = |\vec{q}|$. For heavily doped p-Ge $n(\lambda)$ has not been measured, so we took the data for pure Ge with some broadening for the values above the E_1 gap (~2.3 eV).[19] The broadening of the optical constant of GaAs with doping has been measured for energies above the E_1 gap.[21,22] We assumed for Ge a broadening similar to that measured for GaAs of comparable doping.

The energies of the laser lines used to excite the first-order Raman spectra of Ge lie in the range from 1.83 to 2.71 eV and the wave vector of the phonons created in the Raman process cover a range from $\sim 9\times10^5$ to $\sim 13\times10^5$ cm^{-1}. In Fig. 4 the arrows represent this range for the wave

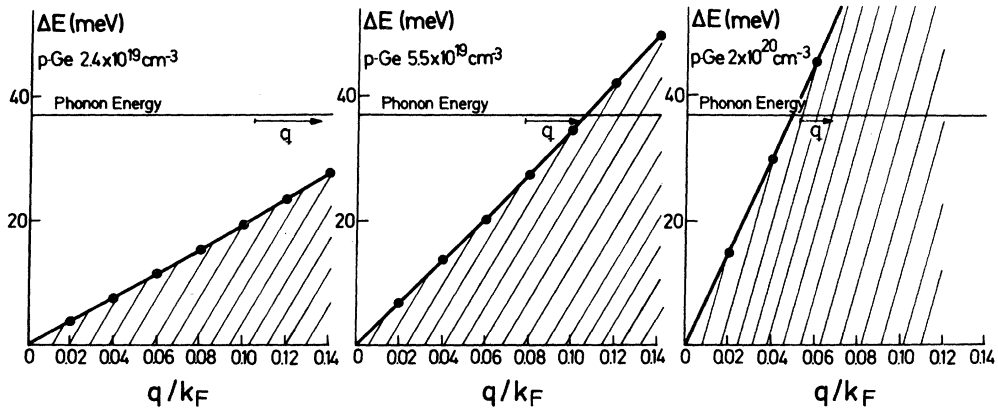

FIG. 4. Free-particle excitations within the heavy-hole valence band of p-Ge (shaded area) and range of the wave vector of the optical phonons created by the Raman process (arrows).

vectors $\vec{q}$ relative to the Fermi wave vector $\vec{k}_F$ for each particular hole concentration. The striped area corresponds to the free-particle excitations within the heavy-hole valence band, which for a given wave vector $\vec{q}$ extends from zero to[23]

$$\Delta E_{\max}(q) = E_F\left(2\frac{q}{k_F}+\frac{q^2}{k_F^2}\right). \tag{10}$$

Equation (10) assumes $T=0$ K and free electrons (holes) in parabolic bands,

$$k_F=(3\pi^2 p)^{1/3} \tag{11}$$

and

$$E_F=\frac{\hbar^2 k_F^2}{2m_v}, \tag{12}$$

with p the free-hole concentration and m_v the heavy-hole mass. We used the value of $m_v=0.34$ in the evaluation of E_F.[24]

The observed dependence of the frequency shifts $\Delta\Omega$ and broadening $\Delta\Gamma$ on the incident laser energy can be explained by considering that the created phonon of wave vector $\vec{q}$—determined by the wavelength of the incident photons through Eq. (9)—decays into the free-particle excitations within the heavy-hole valence band. We neglect the presence of holes in the light-hole valence band as their mass is small compared with m_v.[24] The free-particle excitations take place from occupied states below the Fermi energy to free states above it.

The density of states for these excitations is actually the imaginary part of the Lindhard dielectric function (except for unimportant factors) and can be written as follows[23]:

$$\rho(E')=\frac{m_v^2}{\pi^2\hbar^4}\frac{E'}{q} \tag{13}$$

for $0\leq E'\leq \Delta E_{\max}(q)$ and

$$\rho(E')=0 \tag{14}$$

for $E'>\Delta E_{\max}(q)$. As shown in Eq. (6) the broadening of Raman lines of the heavily doped materials, that is, the decrease of the phonon lifetime due to the electron-phonon coupling, depends on the density of states of the continuum at the energy of the phonon. In order to take into account the finite lifetime of the electronic states at the energy $\hbar\Omega=\Delta E_{\max}(q)$ when $T\neq 0$ K, we convoluted the density of states given by Eqs. (13) and (14) with a Lorentzian curve of linewidth Δq given by

$$E_F 2\frac{\Delta q}{k_F}\simeq kT. \tag{15}$$

The densities of states obtained after the convolution, evaluated at the energy $E'=\hbar\Omega$, are shown in Fig. 5 for the three hole concentrations under study. For 2×10^{20} and 5.5×10^{19} holes cm^{-3} in the range of the wave vectors $\vec{q}$ of the phonons created in the experiment an increase of $\rho(\hbar\Omega)$ takes place with increasing $\vec{q}$. Because of Eq. (6) the Raman lines become more broadened for larger wave vectors $\vec{q}$, that is, for higher energies of the incoming photons, in qualitative agreement with the experimental results listed in Table II. For the sample with 2.4×10^{19} holes cm^{-3} the contribution

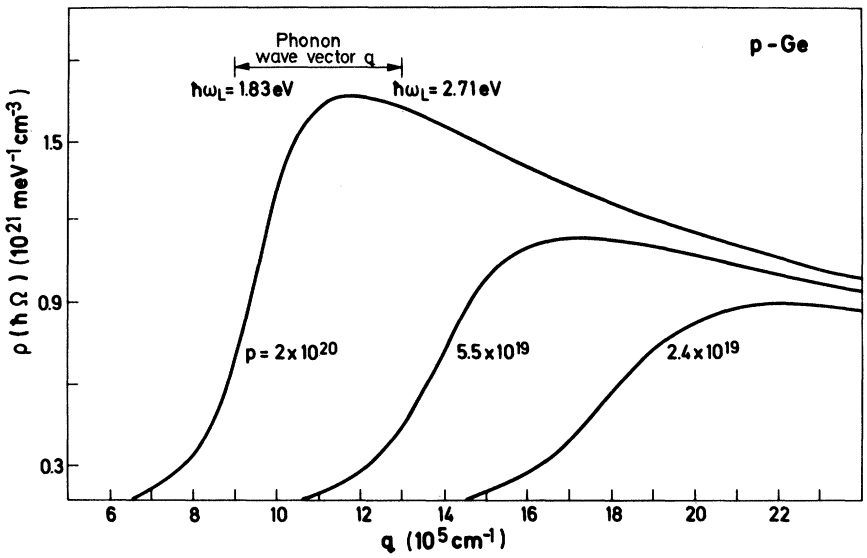

FIG. 5. Density of states of the free-particle excitations as a function of the wave vector $\vec{q}$ for finite temperatures.

to the lifetime of the electronic states due to the finite temperature is not sufficient to explain the $\vec{q}$ dependence of the broadening. However, any other additional smearing of the electronic states, for example, due to fluctuations of the impurity potentials, suffices to explain it qualitatively.

We discuss next the $\vec{q}$ dependence of the frequency shifts using Eq. (5). With the density of states given by Eqs. (13) and (14) the principal part of the integral in Eq. (5) becomes:

$$P\int_0^{\Delta E_{\max}(q)} \frac{\rho(E')}{\hbar\Omega - E'}\,dE' = \frac{m_v^2}{\pi^2\hbar^4 q}\left[\Delta E_{\max}(q) - \hbar\Omega \ln|\hbar\Omega - \Delta E_{\max}(q)| + \hbar\Omega \ln(\hbar\Omega)\right] = P(q) \tag{16}$$

with $\Delta E_{\max}(q)$ given by Eq. (10).

The $P(q)$ evaluated with Eq. (16) as a function of the wave vector $\vec{q}$ is displayed in Fig. 6. One can see that the real part of the self-energy of the phonon frequency shows as a function of $\vec{q}$ two different types of behavior depending on the hole concentrations. For the samples with 2.4×10^{19} and 5.5×10^{19} holes cm^{-3} the intraband continuum pushes the phonons to higher energies for larger $\vec{q}$. $\hbar\Delta\Omega$ becomes smaller in magnitude with increasing wave vector $\vec{q}$ and can even change sign and become positive if the renormalization of the phonon frequency due to the intraband excitations is larger than that due to the possible interband continuum. The shifts of the Raman lines to higher energies with increasing $\vec{q}$ correspond to the physical situations shown in Fig. 4. For these two lower hole concentrations the phonon energy lies always above the continuum. The energy denominators of the second-order perturbation terms are always positive and a repulsion of the phonon lines to higher energies takes place. As displayed in Fig. 6, when $\vec{q}$ increases the real part of the intraband contribution to the self-energy $P(q)$ decreases in the wave-vector range of our interest for the samples with 2×10^{20} holes cm^{-3}, and consequently the Raman lines shift to lower energies as $\vec{q}$ is increased. Figure 4 shows that the range of wave vectors $\vec{q}$ for this hole concentration lies within the free-particle excitation spectrum. Because of the large density of states for energies around $\Delta E_{\max}(q)$, the electronic states above the phonon line will push it to lower energies. In this manner the unusual dependence of the energy positions of the phonon Raman lines on incident photon energy can be qualitatively explained.

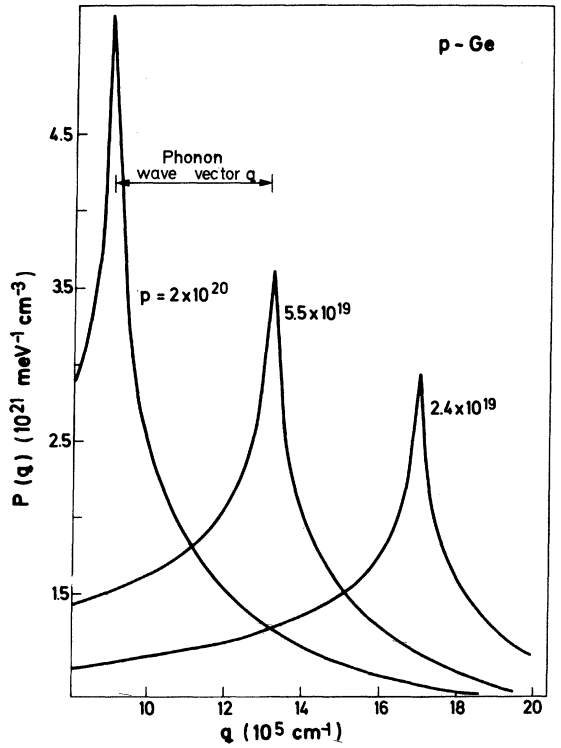

FIG. 6. Wave-vector dependence of the principal value $P(q)$ given by Eq. (16).

In the case of p-Ge we can go even further and try to obtain an estimate of the deformation-potential constant for the electron-phonon interaction. The electronic continuum consists of inter-valence-band as well as intra-valence-band transitions; the latter allow the decay of Raman phonons into free-particle excitations. This decay is not possible in p-GaAs because the heavy-hole mass is approximately 2 times larger than that in Ge. Hence for GaAs the intraband continuum arises only from impurity-induced indirect transitions with the additional complication of the electron-impurity interaction.[8]

We write for the frequency shifts of the optical phonons of p-Ge

$$\hbar\Delta\Omega = \hbar\Delta\Omega_{\text{inter}} + \hbar\Delta\Omega_{\text{intra}}. \tag{17}$$

$\hbar\Delta\Omega_{\text{inter}}$ describes the phonon renormalization due to the interband continuum and can be assumed to be independent of the laser wavelength used to excite the Raman spectra. The second term refers to the coupling of the phonon with the free-particle excitations and can be written using Eqs. (5) and (16) as follows:

$$\hbar\Delta\Omega_{\text{intra}} = V^2 P(q). \tag{18}$$

The matrix element V^2 of the electron-phonon deformation-potential interaction is given by[12]

$$V^2 = \frac{\hbar a_0 d_0^2}{16 M\Omega} g(\vec{k},\vec{q}), \tag{19}$$

where a_0 is the lattice constant, M is the mass of a Ge atom, and d_0 is the deformation-potential constant. The factor $g(\vec{k},\vec{q})$ accounts for the fact that the induced splittings in the electronic band structure due to the phonon vibrations depend on the orientations of the electron wave vector $\vec{k}$ and the phonon wave vector $\vec{q}$. A mean value of $g(\vec{k},\vec{q})$ can be obtained by calculating the matrix elements of the electron-phonon interaction for a given phonon polarization and for different symmetry directions in $\vec{k}$ space. Following the procedure described in Ref. 4 we get for $g(\vec{k},\vec{q})$ a value of $\sim\frac{1}{7}$ (see the Appendix).

The dots of Fig. 7 represent the measured shifts as a function of $\vec{q}$. Equation (9) was used to relate $\vec{q}$ to the wavelength of the incident laser light whereby an error of $\Delta q \simeq 10^5\,\mathrm{cm}^{-1}$ is estimated for $\vec{q} > 12\times 10^5\,\mathrm{cm}^{-1}$. Placing Eqs. (18) and (19) into Eq. (17), theoretical fits to the experimental points were performed using as a fitting parameters $\hbar\Delta\Omega_{\mathrm{inter}}$ and d_0. The solid lines display the best fits obtained, from which the following values were determined: $\hbar\Delta\Omega_{\mathrm{inter}} = -9\ \mathrm{cm}^{-1}$ for 2×10^{20} holes cm^{-3} and $-3\ \mathrm{cm}^{-1}$ for 5.5×10^{19} holes cm^{-3}, respectively. For the deformation-potential constant d_0 we obtained $d_0 = 32 \pm 6$ eV. This value agrees with the previously published ones of +33 eV from band-structure calculations[25] and 27 eV from self-energy studies.[12] It is also in agreement with the values of other semiconductors: $d_0 = +27$ eV for Si (Ref. 12) and +48 eV for GaAs (Ref. 16).

Lawaetz performed a theoretical calculation of the self-energy of the optical phonon of Ge taking into account the detailed electronic band structure of the material.[12] In order to get a reasonable agreement with the experimental data of Cerdeira and Cardona[2] (only one incident photon energy was used) he had to assume the presence of indirect transitions and to introduce them in a cumbersome way into the formalism. His calculation predicted a very strong $\vec{q}$ dependence of the frequency shifts and broadening of the phonon Raman lines of p-Ge. Our measurements confirm these predictions, which we were able to explain with a simplified model.

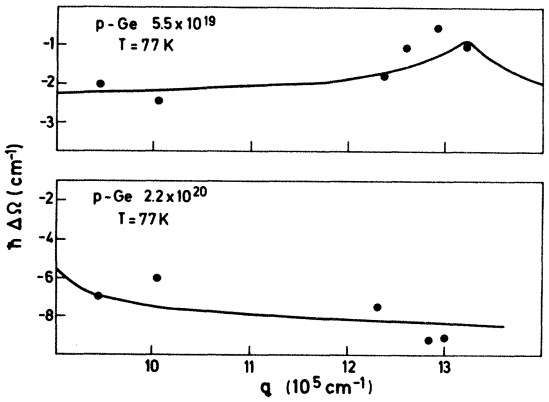

FIG. 7. Wave-vector dependence of the frequency shifts in p-Ge. The dots represent the experimental points and the solid lines theoretical fits, performed as described in the text [see Eq. (17) and following text].

ACKNOWLEDGMENTS

One of us (D.O.) wants to acknowledge helpful discussions with Dr. M. Chandrasekhar and support from the Deutscher Akademischer Austauschdienst. We would also like to thank Mr. E. Kisela for the help in sample preparation as well as the technical assistance of Mr. H. Hirt.

APPENDIX

For $\vec{k}$ near the Fermi wave vector, the valence-band wave functions of the heavy holes can be rep-

TABLE III. Matrix elements of heavy-hole–phonon intraband interaction for different symmetry directions in $\vec{k}$ space.

$\vec{k}$ direction	Multiplicity	$\bar{X}$	$\bar{Y}$	$\bar{Z}$	$\langle\nu\vert\, xy \,\vert\nu\rangle$
[001]	6	$\frac{1}{\sqrt{2}}(x-y)$	$\frac{1}{\sqrt{2}}(x+y)$	z	0
[111]	2	$\frac{1}{\sqrt{2}}(x-y)$	$\frac{1}{\sqrt{6}}(x+y-2z)$	$\frac{1}{\sqrt{3}}(x+y+z)$	$-\frac{1}{3}$
[$\bar{1}$11]	6	$\frac{1}{\sqrt{2}}(y-z)$	$\frac{1}{\sqrt{6}}(2x+y+z)$	$\frac{1}{\sqrt{3}}(-x+y+z)$	$\frac{1}{3}$
[110]	6	$\frac{1}{\sqrt{2}}(-x+y)$	z	$\frac{1}{\sqrt{2}}(x+y)$	$\frac{1}{2}$
[1$\bar{1}$0]	6	$\frac{1}{\sqrt{3}}(x+y+z)$	$\frac{1}{\sqrt{6}}(x+y-2z)$	$\frac{1}{\sqrt{2}}(x-y)$	$\frac{1}{2}$

resented by [12,25]

$$|\nu\rangle = \frac{1}{\sqrt{2}}(\bar{X} + i\bar{Y}) \tag{A1}$$

and the corresponding time-reversed partner. The $\bar{Z}$ axis must lie along to the direction of the wave vector $\vec{k}$; $\bar{X}$ lies along a direction perpendicular to the plane defined by $\bar{Z}$ and the polarization of the phonon, and $\bar{Y}$ is perpendicular to both $\bar{Z}$ and $\bar{X}$. The crystallographic axes will be denoted by x, y, and z.

The symmetry of the zone-center optical phonon in the diamond structure is Γ_{25}, the same as the symmetry of a traceless [111] strain. Thus to evaluate the factor $g(\vec{k},\vec{q})$ of Eq. (19) for the intraband scattering, we have to calculate a mean value of the matrix element

$$|\langle \nu | xy | \nu \rangle|^2 \tag{A2}$$

for different symmetry directions in $\vec{k}$ space [4] (xy represent a function with the same transformation properties as xy under the point-group operations of the cubic group). The values calculated assuming a phonon polarization along the [111] axis, are listed in Table III; from which we obtain

$$\langle |\langle \nu | xy | \nu \rangle|^2 \rangle_{av} = g(\vec{k},\vec{q}) \simeq \tfrac{1}{7}. \tag{A3}$$

[1]For a review see M. Cardona, J. Phys. Soc. Jpn. 49, Suppl. A, 23 (1980).

[2]F. Cerdeira and M. Cardona, Phys. Rev. B 5, 1441 (1972).

[3]M. Chandrasekhar, M. Renucci, and M. Cardona, Phys. Rev. B 17, 1623 (1978).

[4]F. Cerdeira, T. A. Fjeldly, and M. Cardona, Phys. Rev Rev. B 8, 4734 (1973).

[5]D. Guidotti, Shui Lai, M. V. Klein, and J. P. Wolfe, Phys. Rev. Lett. 43, 1950 (1979).

[6]D. Olego, H. Chandrasekhar, and M. Cardona, in *Physics of Semiconductors, 1978,* edited by B. L. H. Wilson (Institute of Physics, Bristol, 1979), p. 1313.

[7]D. Olego and M. Cardona, Solid State Commun. 32, 375 (1979).

[8]D. Olego, M. Cardona, and U. Rössler, Phys. Rev. B 22, 1905 (1980).

[9]S. M. Sze, *Physics of Semiconductor Devices* (Wiley-Interscience, New York, 1969).

[10]The selection rules are quoted for example by W. Richter, in *Solid State Physics,* Vol. 78 of *Springer Tracts in Modern Physics,* edited by G. Höhler (Springer, Berlin, 1976), p. 121.

[11]R. W. Keyes, in *Solid State Physics,* edited by F. Seitz and D. Turnbull (Academic, New York, 1967), Vol. 20, page 37.

[12]P. Lawaetz, *The Influence of Holes on the Phonon Spectrum of Semiconductors* (Physics Laboratory III, The Technical University of Denmark, Lyngby, 1978).

[13]A. Pinczuk and E. Burstein, in *Light Scattering in Solids,* edited by M. Cardona (Springer, Berlin, 1975), p. 23.

[14]U. Fano, Phys. Rev. 124, 1866 (1961).

[15]R. Trommer and M. Cardona, Phys. Rev. B 17, 1865 (1978).

[16]M. Grimsditch, D. Olego, and M. Cardona, Phys. Rev. B 20, 1758 (1979).

[17]M. Cardona, F. Cerdeira, and T. A. Fjeldly, Phys. Rev. B 10, 3433 (1974).

[18]D. Olego and M. Cardona, Phys. Rev. B 22, 886 (1980).

[19]M. Cardona, *Modulation Spectroscopy* (Academic, New York, 1969), p. 63.

[20]F. Cerdeira, W. Dreybrodt, and M. Cardona, Solid State Commun. 10, 591 (1972).

[21]E. Vigil, J. Rodriguez, and R. Perez Alvarez, Phys. Status Solidi B 90, 409 (1978).

[22]D. Aspnes, in *Optical Properties of Solids: New Developments,* edited by B. O. Seraphin (North-Holland, Amsterdam, 1976), p. 799.

[23]D. Pines, in *Elementary Excitations in Solids* (Benjamin, New York, 1963).

[24]C. Kittel, *Introduction to Solid State Physics,* 5th ed. (Wiley, New York, 1976), and references therein.

[25]M. Cardona, in *Atomic Structure and Properties of Solids,* edited by E. Burstein (Academic, New York, 1972), p. 514.